Calorimetric and spectroscopic investigation of the unfolding of human apolipoprotein B

Mary T. Walsh and David Atkinson

Department of Biophysics, Housman Medical Research Center, Boston University School of Medicine, 80 East Concord Street, Boston, MA 02118-2394

Abstract The unfolding of human apolipoprotein B-100 in its native lipid environment, low density lipoprotein (LDL), and in a soluble, lipid-free complex with sodium deoxycholate (NaDC) has been examined using differential scanning calorimetry (DSC) and near UV circular dichroic (CD) spectroscopy. High resolution DSC shows that LDL undergoes three thermal transitions. The first is reversible and corresponds to the order-disorder transition of the core-located cholesteryl esters (CE) (T_m = 31.1°C, ΔH = 0.75 cal/g CE). The second, previously unreported, is reversible with heating up to 65°C (T_m = 57.1°C, ΔH = 0.20 cal/g apoB) and coincides with a reversible change in the tertiary structure of apoB as shown by near UV-CD. No alteration in the secondary structure of apoB is observed over this temperature range. The third transition is irreversible (T_m = 73.5°C, ΔH = 0.99 cal/g apoB) and coincides with disruption of the LDL particle and denaturation of apoB. The ratio of $\Delta H/\Delta H_{vH}$ for the reversible protein-related transition suggests that this is a two-state event that correlates with a change in the overall tertiary structure of the entire apoB molecule. The second protein-related transition is complex and coincides with irreversible denaturation. ApoB solubilized in NaDC undergoes three thermal transitions. The first two are reversible (T_m = 49.7°C, ΔH = 1.13 cal/g apoB; T_m = 56.4°C, ΔH = 2.55 cal/g apoB, respectively) and coincide with alterations in both secondary and tertiary structure of apoB. The changes in secondary structure reflect an increase in random coil conformation with a concomitant decrease in β-structure, while the change in tertiary structure suggests that the conformation of the disulfide bonds is altered. The third transition is irreversible (T_m = 66.6°C, ΔH = 0.54 cal/g apoB) and coincides with complete denaturation of apoB and disruption of the NaDC micelle. The ratio of $\Delta H/\Delta H_{vH}$ for the two reversible transitions indicates that each of these transitions is complex which may suggest that several regions or domains of apoB are involved in each thermal event.—**Walsh, M. T., and D. Atkinson.** Calorimetric and spectroscopic investigation of the unfolding of human apolipoprotein B. *J. Lipid Res.* 1990. **31:** 1051–1062.

Supplementary key words differential scanning calorimetry • circular dichroism • low density lipoprotein • sodium deoxycholate micelles • cholesteryl esters

Low density lipoprotein (LDL) is the major transport particle for cholesterol in human plasma (1). Physical techniques have provided a model of LDL as being a microemulsion containing a neutral lipid core of cholesteryl esters and triglyceride that is surface-stabilized by a monolayer of polar phospholipids, cholesterol, and apolipoprotein B (apoB) (2–4). ApoB, the structural protein of LDL, also plays a critical physiological role in the transport and delivery of cholesterol and is the ligand for the receptor-mediated uptake and clearance of LDL from the circulation (5, 6).

ApoB has a molecular weight of ~550,000 and is monomeric (one of the largest monomeric proteins known) (7–9). The primary sequence of amino acids has been inferred from cDNA clones and glycosylation sites have been predicted by computer-aided analysis and, recently, determined by chemical methods (10). Although the primary sequence of apoB is now known and the functional and structural domains of apoB that determine both LDL structure and metabolism are beginning to emerge (9, 10), the detailed organization of apoB on the surface of LDL remains to be elucidated.

The low resolution calorimetric behavior of LDL has been reported extensively (2, 3). At a protein concentration of 25 mg/ml, LDL has been shown previously to undergo two thermal transitions (2, 3). The first transition, associated with the reversible order-disorder transition of the core-located cholesteryl esters, encompasses body temperature. The second irreversible transition was associated with disruption of the LDL particle and protein unfolding-denaturation over the temperature range 70–90°C. In addition, the low resolution calorimetric behavior of apoB solubilized in sodium deoxycholate (NaDC) has been reported previously (11). ApoB solubilized in NaDC (1.8 mg/75 μl = 24 mg apoB/ml) was shown to undergo an irreversible endothermic transition

Abbreviations: T_m, temperature of the maximum of the change in heat capacity; LDL, low density lipoprotein; apoB, apolipoprotein B-100; DSC, differential scanning calorimetry; CD, circular dichroism; ΔH, calorimetric enthalpy; ΔH_{vH}, van't Hoff enthalpy; NaDC, sodium deoxycholate; C_p, heat capacity; CE, cholesteryl ester; T_o, onset temperature; T_e, end temperature.

over the temperature range 47 to 64°C with a T_m of 52°C. The shape of this peak was observed to be quite asymmetric.

Circular dichroic (CD) spectroscopy, far and near UV, provides both secondary and tertiary structural information on protein conformation. Measured as a function of temperature, structural changes between conformational states may be correlated with folding-unfolding events and thermodynamic parameters provided by the calorimetry experiments. Previous analyses of far UV CD spectra for elements of secondary structure of apoB in LDL (11) have shown that from 0 to 70°C the secondary structure of apoB is not altered and contains ~40% α-helix, 20% β-sheet, and 40% random coil. ApoB in NaDC micelles has a secondary structure similar to apoB in LDL over the temperature range 5 to 30°C. Between 30 and 60°C reversible changes in secondary structure occur, particularly regarding the β-sheet versus random coil components, with α-helix decreasing only slightly to ~38% (11). Thus, unlike apoB in LDL, the secondary structure of apoB solubilized in NaDC is responsive to alteration in temperature and undergoes reversible conformational changes over a temperature range where a calorimetric event is also observed.

High resolution adiabatic calorimetry (12, 13) allows the use of relatively dilute solutions (<2 mg/ml compared to ~25 mg/ml for conventional calorimetry), thus reducing the potential for concentration-dependent protein aggregation. Heating rates used in this technique are more directly comparable to those used in other physical methods such as CD. We report here a more detailed structural and thermodynamic description of the unfolding-denaturation of apoB in LDL and solubilized in NaDC. The calorimetry data has been obtained at higher resolution than data presented in previous reports (2, 3, 11). These data combined with our previous results from far UV CD studies and the new near UV CD experiments provide insights into both the secondary and tertiary structural organization of apoB in detergent solution and in its native lipid environment.

EXPERIMENTAL PROCEDURES

Materials

All chemicals were standard reagent grade unless otherwise indicated. Sodium deoxycholate (NaDC) was purchased from Calbiochem (La Jolla, CA) and twice recrystallized from 80% ethanol.

Methods

Plasma was obtained from freshly drawn blood from normal volunteers. For the current studies the number of plasma donors was limited to two members of our own laboratory whose LDL had been shown to contain only the B-100 form of apoB (14). Disodium ethylenediaminetetraacetic acid (EDTA) and sodium azide (NaN_3) were added to the freshly drawn plasma to final concentrations of 0.01% and 0.02%, respectively. LDL was isolated by repetitive ultracentrifugation between salt densities of 1.025 and 1.050 g/ml (addition of solid KBr) (15). Isolated LDL was washed by ultracentrifugal flotation through an overlayering solution of d 1.050 g/ml KBr, 0.02% NaN_3. All spins were performed at 55,000 rpm in a Beckman L8-70 ultracentrifuge in a 70 Ti rotor for 16 h at 4°C. Purity of LDL from other lipoprotein fractions was verified by agarose electrophoresis (16) by staining with Sudan Black B and Coomassie Brilliant Blue.

Solubilization of LDL and isolation of apoB

The free sulfhydryl group on apoB of LDL was blocked by interaction of LDL with iodoacetamide (17). LDL was then dialyzed against 50 mM sodium chloride, 50 mM sodium carbonate, 0.02% NaN_3, pH 10 (standard buffer).[1] Disruption and solubilization of the molecular components of LDL was achieved with NaDC as described previously (18). After incubation with NaDC, fractionation was carried out by gel filtration chromatography on Sepharose CL-4B with an elution buffer containing 10 mM NaDC in standard buffer. ApoB was recovered in high yield and was free of lipid. Protein-containing fractions were pooled and concentrated to 2 mg of protein/ml by ultrafiltration (Amicon YM-10 filters; Amicon Corp., Danvers, MA) and stored at 4°C.

The structural integrity of apoB was verified prior to physical chemical measurements by SDS-polyacrylamide gradient gel electrophoresis (3-24) (19). LDL was used within 1 week of isolation by centrifugation. ApoB solubilized in NaDC was used up to 2 weeks after purification.

Analytical methods

Protein concentration was estimated by the method of Lowry et al. (20) utilizing the modification of Markwell et al. (21) which incorporates 1% SDS in both bovine serum albumin standard and samples.

Techniques of sample preparation

LDL (~10 mg protein/ml, 2 ml total volume) was dialyzed exhaustively against the standard buffer at 4°C.

[1]The presence and localization of two intramolecular thiolester linkages in apoB have recently been reported (50, 51). These investigators utilized preparative methods that are very different from those used in our current studies, and reported by ourselves and others previously (11, 18, 52). Our methods were selected to maintain the structural integrity of apoB and for gentleness and thoroughness in delipidation and solubilzation of apoB. Acetylation of apoB of LDL was accomplished by the method of Hirs (53). After preparation, no free sulfhydryl groups were detected and no degradation or aggregation of apoB was detected on SDS-PAGE gradient gels. We have not performed analyses on our LDL and apoB-NaDC preprations to determine whether or not thiolester bonds are present in apoB.

ApoB solubilized in NaDC was dialyzed exhaustively against the standard buffer plus 10 mM NaDC at 4°C.

Circular dichroism

CD spectra were recorded in continuous scanning mode from 250 to 200 nm (far UV) and from 320 to 270 nm (near UV) with a Cary Model 61 CD Spectropolarimeter (Varian, Palo Alto, CA) calibrated from 500 to 190 nm with *d*-10-camphorsulfonic acid (1 mg/ml in ethanol). Spectra were recorded over the temperature range 5–70°C. The sample temperature was maintained by circulating ethylene glycol–water through the sample compartment by means of a thermostatted refrigerator–heater bath (Neslab, Inc., Portsmouth, NH). Temperature was measured to within 0.1°C by means of a copper constantan thermocouple positioned in contact with the CD cell in the sample compartment. Samples were allowed to equilibrate for 30 min in the sample compartment at each temperature prior to recording the spectra. For far UV CD spectra (250–200 nm), 0.1-cm or 0.02-cm quartz cuvettes were used with a protein concentration of 0.03–0.3 mg/ml.[2] For near UV CD spectra (270–320 nm), a 1-cm quartz cuvette was used with a protein concentration of 2–5 mg/ml.

All spectra reported are the average of three individual spectra on three to four different samples and have been corrected for baseline contributions (11). Values for trough depth were read at 1-nm intervals for each spectrum and a mean value for the trough depth at each wavelength was obtained. Molar ellipiticity (degrees-cm^2/mol) was calculated according to standard equations (22–24).

Calorimetry

High resolution calorimetry was conducted on an MC-2 calorimeter (MicroCal Inc., Amherst, MA) which contains matched Tantalum sample and reference cells (volume = 1.202 ml). The calorimeter is interfaced to an IBM PC via a DT-2801 A/D conversion board (Analog Devices, Marlboro, MA) which allows automated data collection and analysis. Samples were exhaustively dialyzed at 4°C against the appropriate buffer. Prior to introduction into the calorimeter cells, both dialysate and protein were thoroughly degassed under vacuum (without stirring for protein-containing samples) at room temperature. The reference solution (dialysate), protein sample, and calorimeter cells were at room temperature at the time of sample introduction, and subsequently cooled. For LDL, a typical concentration was ~6 mg protein/ml. For apoB solubilized in NaDC, a typical concentration was ~2 mg/ml.

Calorimetric measurements were recorded over the temperature range 0–5° to 60°C and 0–5°C to 100°C at heating rates of 90°C/h (1.5°C/min) or 45°C/h (0.75°C/min). Each sample was heated and cooled two to five times. All measurements were performed under nitrogen pressure to avoid vaporization of solvent during high temperature heating.

Buffer–buffer or water–water baselines were subtracted from buffer–sample scans. Analysis and evaluation of data for calorimetric enthalpy (ΔH) values from the heat capacity versus temperature curves and van't Hoff enthalpy (ΔH_{vH}) values were performed using the software provided with the MC-2. This analysis uses the methodology and theoretical framework described by Freire and Biltonen (25–27) and Rigell, de Saussure, and Freire (28). The T_m for a given transition was taken to be the point of maximum excess heat capacity. The ΔH was calculated from the area under each calorimetric peak. Numerical integration of peak areas and resolution of overlapping peaks were performed using curve-fitting procedures utilizing either linear baselines (13) or sigmoidal ("spline") baselines (29) when a change in heat capacity of the sample accompanied the thermal transitions. Heat capacity profiles were subjected to deconvolution analysis as described by Freire and Biltonen (25–27) and Privalov (12). This type of analysis was applied to sequential transitions according to the guidelines of Rigell et al. (28) and utilizing DECONV software supplied with the MC-2.

The ratio of the calorimetric to van't Hoff enthalpy ($\Delta H/\Delta H_{vH}$) was calculated according to the formula (30),

$$\Delta H/\Delta H_{vH} = \Delta H^2/C_{p'max}4RT_m^2$$

where ΔH is the calorimetric enthalpy, $C_{p'max}$ is the maximum in the heat capacity function, R is the gas constant, and T_m is the transition temperature. This ratio is 1 if the transition is from one state to another (two-state type), greater than 1 if more than two states are involved, and may be less than 1 in certain cases if the process is irreversible (30–32).

The molecular weight of apoB used for calculation of molar quantities was M_R 550,000. This value reflects the molecular weight contribution from the 4536 amino acid residues (7–9) plus carbohydrate (33–36).

RESULTS

High resolution calorimetry of low density lipoprotein

High resolution calorimetry of LDL shows that the particle undergoes a series of thermal events. Calorimetric analysis was performed on ten different LDL samples from three different LDL preparations. A representative example is presented in **Fig. 1**. Mean thermodynamic data from the results of all ten samples are presented in **Table 1**.

[2]These spectra were recorded as control experiments for the calorimetry samples, and were compared to our previously published data (11, 18). Thus, the spectra are not reported in this manuscript.

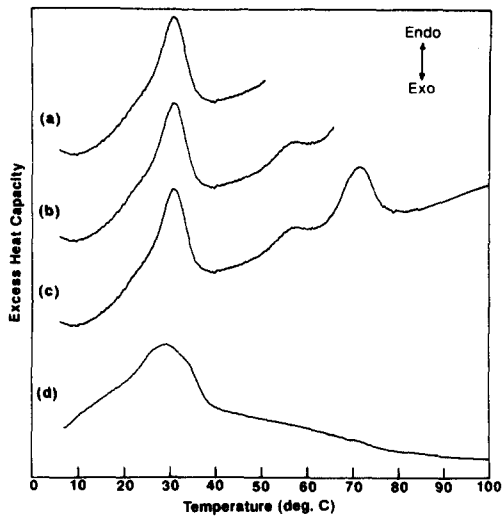

Fig. 1. High resolution calorimetry of low density lipoprotein. LDL was dialyzed exhaustively against the standard buffer at 4°C prior to calorimetry. LDL (1.202 ml) containing 7.2 mg apoB, 15.1 mg cholesteryl ester was placed in the sample cell. The reference cell contained the dialysate buffer. Heating rate was 90°C/h for a–d. Buffer-buffer baselines were subtracted from each of the scans. The data were not normalized to either the number of mol of CE or apoB in the sample cell. For complete analysis of the data and quantitation with respect to CE mass and the mass and number of molecules of apoB, see the text and Table 1. LDL was heated from (a) 0–50°C; (b) 0–65°C; (c) 0–100°C; (d) 0–100°C, second heating.

Heating from 0 to 50°C shows that LDL undergoes one endothermic transition (Fig. 1a) which exhibits an asymmetry on the low temperature side of the main peak and has a T_m of ~31°C and ΔH ~0.75 cal/g CE. This transition corresponds to the well-characterized, reversible order-disorder transition of the core-located cholesteryl esters, described previously by others (2, 3).

On heating to 65°C, LDL undergoes an additional transition that has a low enthalpy (ΔH ~0.20 cal/g apoB) and a T_m of ~57°C (Fig. 1b). Since none of the lipid components of LDL are known to undergo a thermal transition over this temperature range, the enthalpy for this transition is expressed in terms of the mass of protein. This previously unreported thermal event is reversible upon repeated heatings to 65°C. Reduction of the heating rate to 45°C per h does not alter either the transition temperature or enthalpy of this event (not shown).

Upon heating to 100°C, (Fig. 1c) in addition to the two reversible thermal transitions described above, LDL undergoes a third transition at a T_m of ~73°C with ΔH ~1.0 cal/g apoB. This corresponds to irreversible unfolding-denaturation and thermal disruption of the LDL particle as reported by Deckelbaum et al. (2, 3). Repeated scans of LDL show the thermal behavior illustrated in Fig. 1d, with a single broad transition and a T_m of ~30°C and ΔH = 0.70 cal/g CE, corresponding to cholesteryl esters that are no longer restricted in their melting due to particle constraints and that are free to melt in a cooperative manner.

TABLE 1. Summary of thermodynamic data for low density lipoprotein

Heating Sequence	T_m, CE	ΔH	T_m, ApoB	ΔH		$\Delta H_{v,H}$	$\Delta H/\Delta H_{v,H}$
	$[T_o, T_f]$ T_m[a,b]	cal/g CE	$[T_o, T_f]$ T_m	cal/g ApoB	kcal/mol ApoB	kcal/mol ApoB	
0–50°C	[15.6 ± 0.4, 39.4 ± 0.2] 31.1 ± 0.3	0.75 ± 0.6					
0–65°C	----	---	[48.5 ± 2.0, 62.7 ± 0.6] 57.1 ± 0.5	0.20 ± 0.002	110 ± 11	108 ± 20	1.02:1
0–100°C			(1) [48.5 ± 2.0, 62.7 ± 0.6] 57.1 ± 0.5	0.20 ± 0.002	110 ± 11	108 ± 20	1.02:1
			(2) [63.8 ± 1.0, 81.1 ± 3.4] 73.5 ± 4.7	0.99 ± 0.10	545 ± 55	118 ± 42[c]	4.61:1[c]
Second, 0–100°C	[14.9 ± 1.8, 40.4 ± 1.8] 29.9 ± 0.4	0.70 ± 0.04					

All temperatures are in °C.
[a] T_m and ΔH values are the average of data from 10 samples.
[b] Mean ± 1 standard deviation.
[c] $\Delta H/\Delta H_{v,H}$ are reported for this thermal event for comparison only since this transition is irreversible.

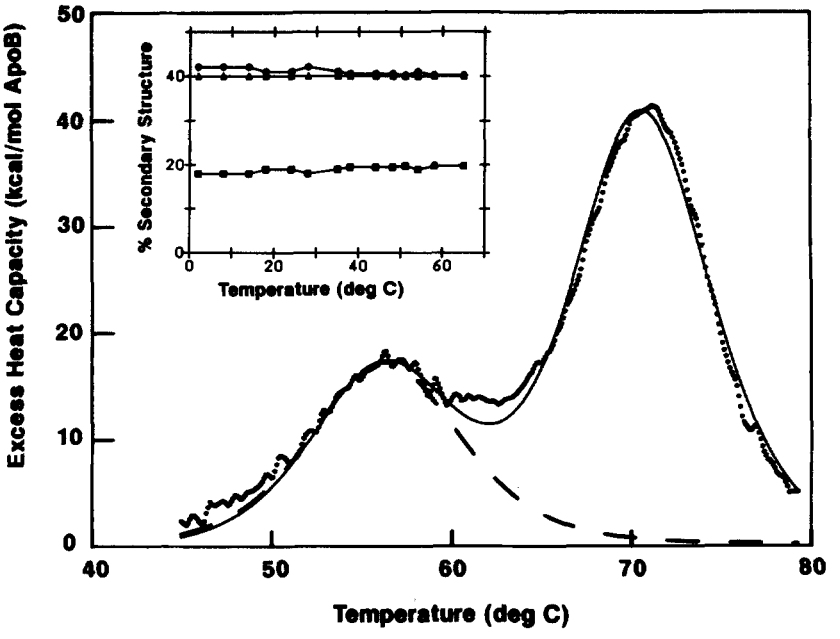

Fig. 2. Deconvolution of the heat capacity function for apoB in LDL. Original calorimetric data that have been baseline-corrected (dotted line with variation); theoretical best-fit curve for the raw data (standard deviation of fit = 0.3%) (smooth solid line); peak resulting from the deconvolution analysis of the first reversible peak (dashed line). For the two protein-related transitions, the method described by Krishnan and Brandts (13) was used to establish the baseline between 45 and 80°C. For the first peak, deconvolution analysis was performed to fit the maximum number of two-state transitions that best approximated this reversible transition. The second peak was irreversible and was therefore excluded from deconvolution analysis. Inset: data replotted from ref. 11; (●—●) percentage of α-helix; (■—■) β-structure; (▲—▲) random coil for apoB in LDL.

Fig. 2 shows the data fit for the two transitions assigned to apoB in LDL over the temperature range 45–80°C, together with the thermodynamic deconvolution analysis for the first reversible transition centered at 57°C. As indicated in the data of Table 1, $\Delta H/\Delta H_{vH}$ for the first reversible transition is ~1, indicating that this transition is of the two-state type, and thus probably involves a cooperative structural reorganization of the entire apoB molecule. The irreversible nature of the second transition centered at 71°C suggests that a number of events occur simultaneously (e.g., the unfolding–denaturation of apoB or domains of apoB, disruption of the LDL particles, lipid–protein reorganizations, high temperature phase changes of lipids, etc.).

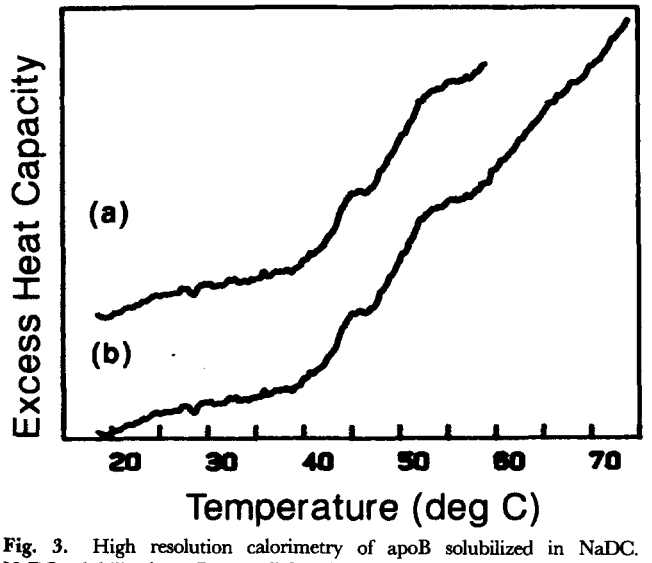

Fig. 3. High resolution calorimetry of apoB solubilized in NaDC. NaDC-solubilized apoB was dialyzed exhaustively against the standard buffer plus 10 mM NaDC at 4°C prior to calorimetry. ApoB-NaDC solution (1.202 ml) (1.8 mg of apoB) was placed in the calorimeter cell. Reference cell contained the NaDC dialysate. Heating rate was 90°C/h. Buffer baselines have been subtracted from each scan. Data have not been normalized to either the mass or number of molecules of apoB in the sample cell. For complete analysis, see text and Table 2; (a) 18–58°C; (b) 18–80°C.

High resolution calorimetry of apoB solubilized in NaDC

Calorimetric analysis was performed on ten different samples of apoB solubilized in NaDC, isolated from three different preparations of LDL. A representative example is presented in **Fig. 3**. The mean data from results of all 10 samples are presented in **Table 2**.

The high resolution calorimetric behavior of apoB solubilized in NaDC is characterized by an overall increase in heat capacity. Subtraction of water or buffer baseline scans from the scans of solubilized apoB does not alter the slope or compensate for the constant increase in heat capacity observed over the temperature range examined. A similar observation has been made in the calorimetric analyses of apoA-I and apoE (37).

Fig. 3 illustrates typical high resolution calorimetric data for apoB solubilized in NaDC over the temperature range 18–80°C. These data are also shown in **Fig. 4** after compensation for the continuous change in specific heat using a spline-fitted baseline between 35 and 70°C (25–28). Initial heating from 0 to 60°C (shown plotted from 18 to 58°C in Fig. 3a) is characterized by two reversible calorimetric transitions (T_m ~49°C, ΔH ~1.0 cal/g apoB; T_m ~56°C, ΔH = 2.5 cal/g apoB). Repeated heating and cooling between 0 and 60°C, as well as decreasing the heating rate to 45°C/h (0.75°C/min) does not alter either the temperature or the enthalpy of these transitions (not shown). Further heating to 100°C (illustrated from 18 to 80°C in Figs. 3b and 4) shows another

TABLE 2. Summary of thermodynamic data for apoB solubilized in NaDC

	T_m[a,b]	ΔH		ΔH_{vH}	
	[T_o,T_c] T_m	cal/g	kcal/mol	kcal/mol	$\Delta H/\Delta H_{vH}$
Peak 1	[43.5 ± 4.3;52.8 ± 5.8] 49.7 ± 4.6	1.13 ± 0.14	622 ± 77	158 ± 19	3.9:1
Peak 2	[50.3 ± 2.9;59.7 ± 4.6] 56.4 ± 1.9	2.55 ± 0.19	1403 ± 105	183 ± 19	7.7:1
Peaks resulting from deconvolution analysis of peaks 1 and 2 of Fig. 3a.					
1	44.9		567		
2	49.5		385		
3	52.5		324		
4	52.8		405		
5	53.3		344		
Peak 3	[61.8 ± 4.0;73.1 ± 4.2] 66.6 ± 3.5	0.54 ± 0.23	297 ± 127	181 ± 22[c]	1.6:1[c]

All cited temperatures are in °C.
[a]Mean ± standard deviation.
[b]T_m and ΔH values are the average of data from 10 samples.
[c]$\Delta H/\Delta H_{vH}$ are reported for this thermal event for comparison only since this transition is irreversible.

peak with T_m of ~65°C and relatively low enthalpy (ΔH ~ 0.54 cal/g apoB). Repeated heatings after the initial heating to 100°C, show that all of the peaks have disappeared, suggesting that either the protein has unfolded irreversibly or the micellar apoB-NaDC complexes are disrupted (or both).

The presence of multiple discrete transitions (both calorimetrically reversible and irreversible) suggests that specific regions or domains of apoB may be melting or "unfolding" at specific temperatures, indicating that when solubilized in NaDC, some regions of the large apoB molecule may be thermodynamically more stable than others.

Thermodynamic deconvolution analysis was carried out on the data shown in Fig. 3 after spline baseline correction as shown in Fig. 4. The two lower temperature peaks were analyzed together since they are both reversible. The third peak was baseline-fitted separately and because of its irreversible nature was not analyzed further. As indicated in Table 2, the first reversible transition has $\Delta H/\Delta H_{vH}$ of ~4, the second ~8, indicating that these reversible thermal events do not represent individual, simple two-state transitions (12, 31, 32). Therefore, these reversible transitions were subjected to thermodynamic deconvolution analysis. The deconvolution analysis (Fig. 4 and Table 2) suggests that the first reversible peak is pre-

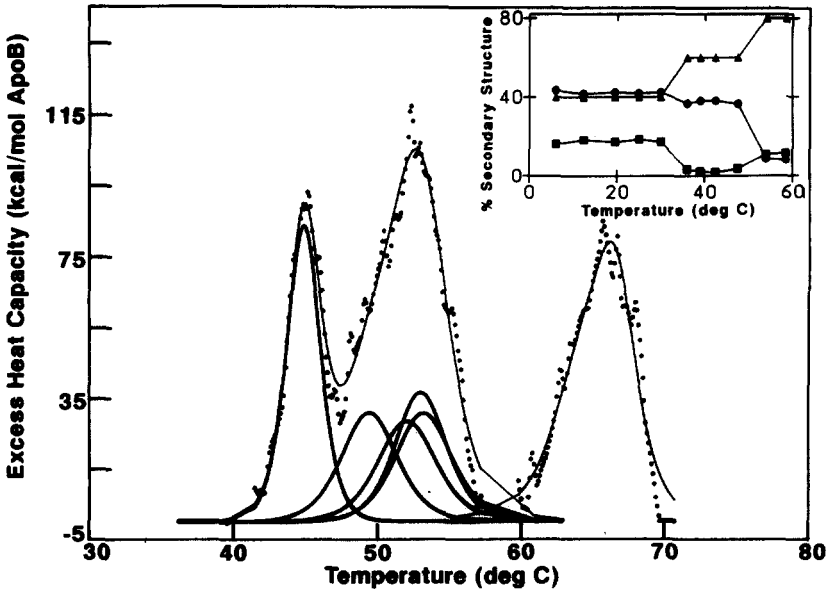

Fig. 4. Deconvolution of the heat capacity function for apoB solubilized in NaDC. Original calorimetric data that has been baseline-corrected (dotted line with variation); theoretical best fit curves for the two lower temperature-reversible peaks (standard deviation of fit = 0.5%) and the higher temperature-irreversible peak (standard deviation of fit = 1.4%) (narrow solid line); peaks resulting from deconvolution analysis of the two lower temperature-reversible peaks (heavy solid line). A sigmoidal baseline was fit between two temperatures by "splines" (29). For these two reversible transitions, deconvolution analysis was performed to find the maximum number of two-state thermal events represented by the two peaks. For the higher temperature transition, deconvolution analysis was not performed because the transition is irreversible. Inset: data replotted from ref. 11; (●—●) percentage of α-helix; (■—■) β structure; (▲—▲) random coil as a function of temperature for apoB in NaDC micelles.

dominated by one major transition with T_m = 44.9°C, comprising 28% of the total ΔH of both reversible transitions. Small portions of the onset regions of two other peaks overlap this first peak. This suggests that a major portion of the apoB molecule (perhaps one specific region or domain) is undergoing a conformational rearrangement independently from most of the other regions of the molecule in a two-state process, with other domains contributing to some extent, thereby elevating the $\Delta H/\Delta H_{vH}$ ratio to 4. The second reversible event centered at 52.7°C is composed predominantly of four independent two-state transitions, all with similar enthalpy (Table 2). Of these four transitions, one has a T_m at 49.5°C while the three other events have very similar T_ms (52.5, 52.8, 53.3°C). The transition at 49.5°C overlaps the most with the lowest peak at 44.9°C. Because of the nature of the high temperature irreversible transition of T_m 65°C, ΔH = 0.85 cal/g, the transition was not analyzed further by deconvolution analysis. All of these data suggest that apoB solubilized in NaDC undergoes a number of reversible thermal events over discrete temperature ranges prior to irreversible denaturation.

Near UV CD studies

To monitor changes in the tertiary structure of apoB in LDL and solubilized in NaDC as a function of temperature, particularly structure involving the aromatic amino acids Trp, Tyr, and Phe, and the disulfide bonds (38), we measured their near UV-CD spectra. The wavelength and ellipticity data are summarized in **Table 3**.

ApoB in LDL

Near UV-CD spectra of LDL were recorded as a function of temperature at 3-4°C increments from 5 to 64°C. Measurements were not made at temperatures above 64°C since the thermal disruption of LDL particles and concomitant release of the core-located CEs and aggregation of apoB produces significant sample turbidity. **Fig. 5** shows selected near UV-CD spectra of LDL recorded at the temperatures indicated. From 5°C (Fig. 5a) to 34°C the curves are similar, with a positive maximum at 290 nm and similar molar ellipticity (**Fig. 6**). From 39 to 55°C the positive maximum, also at 290 nm, has a slightly greater magnitude. Between 55 and 60°C, the magnitude of this positive maximum at 290 nm increases. At 60°C a shoulder is also observed on the main peak between 295 and 300 nm. At 64°C, only one broad positive peak is seen with its maximum shifted to 287 nm and a decreased molar ellipticity at 290 nm. To characterize these changes, the molar ellipticity at 290 nm is plotted as a function of temperature in Fig. 6.

ApoB solubilized in NaDC

Near UV-CD spectra of apoB solubilized in NaDC were recorded as a function of temperature at 3-4°C increments over the temperature range 4 to 72°C. **Fig. 7** shows near UV-CD spectra of apoB solubilized in NaDC recorded at the temperatures indicated. At 7°C (Fig. 7a) the spectrum exhibits a negative minimum from 278 to 282 nm. Near UV-CD spectra recorded from 4 to 40°C are similar to those measured at 7°C, suggesting that over this temperature range no alteration in the tertiary structure of apoB is occurring. This temperature range coincides with that of the relatively featureless region of the calorimetric profile of apoB solubilized in NaDC.

At 42°C, the shape of the spectrum changes. The negative minimum at 272 nm is now accompanied by a shoulder at 280 nm. At 49°C, the negative minimum at 272 and a shoulder at 282-284 nm are still evident; however, their magnitude is diminished. At 55°C, the peak broadens with a minimum over the range 270-280 nm, and a shoulder from 285-290 nm. If the temperature is reversed to 7°C from 55°C or less, the original spectrum

TABLE 3. Wavelength and ellipticity values for peak minima and maxima in the near UV-CD spectra of apoB in LDL and solubilized in NaDC

	T,°C	λmin, max	$[\Theta]_\lambda$ deg-cm²/dmol × 10^{-3}
LDL	5-34	290	+ 21.0
	34-55	290	+ 29.0
	60	290	+ 41.0
		298 (shoulder)	+ 9.0
	64	287	+ 49.0
NaDC	7	278-282	- 35.53
	42	272-274	- 37.40
		280 (shoulder)	- 29.92
	49	272	- 33.66
		282-284	- 24.31--26.20
	55	270-282 (broad)	- 31.79
	64	270	- 31.79
		280-290 (gradual decrease in magnitude)	- 24.31--16.83

LDL: position of maximum shifts only 2-3 nm over the entire temperature range; the major alteration is the magnitude of the maximum and development of a shoulder at 298 nm at temperatures greater than or equal to 60°C.

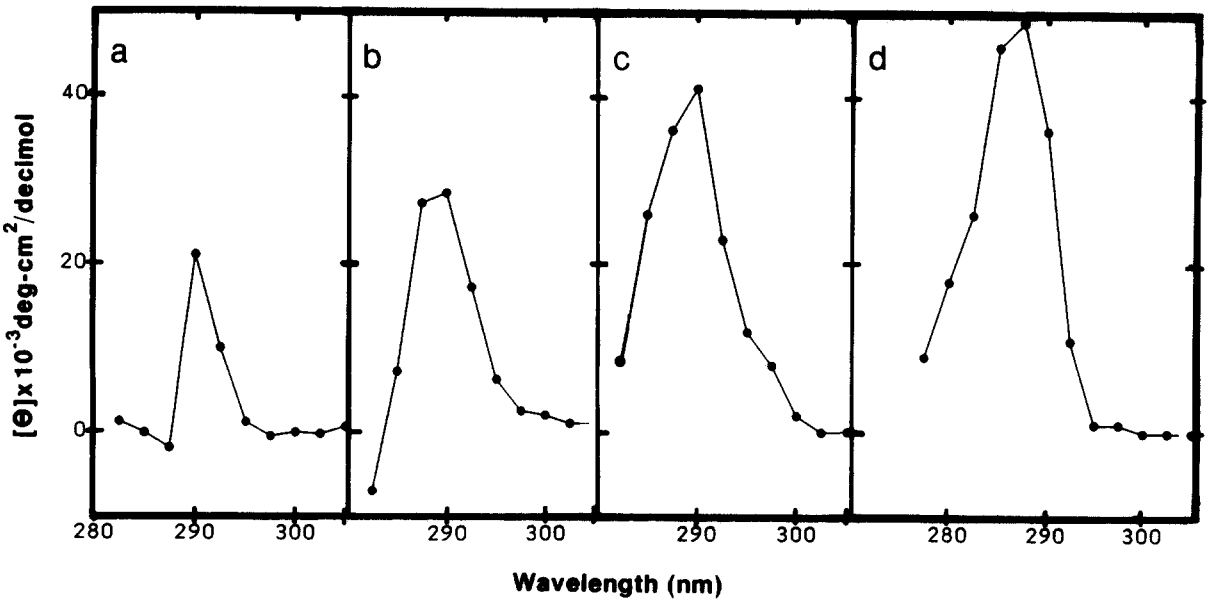

Fig. 5. Near UV circular dichroic spectra of apoB in LDL. LDL samples were ~5 mg of apoB/ml in 50 mM NaCl, 50 mM sodium carbonate, 0.02% NaN_3, pH 10. Cell pathlength was 1.0 cm. *All near UV-CD spectra were recorded from 320 to 260 nm. The data, however, are reported only from 305 to 280 since, at wavelengths greater than 305 nm, the molar ellipticity values were zero, suggesting that no absorptions were occurring over these wavelengths and merely reflected baseline zero values (see Methods for experimental details); (a) 5→34°C (identical); (b) 39→55°C (identical); (c) 60°C; (d) 64°C.

at 7°C returns (not shown), indicating that any alteration in the tertiary structure of apoB over this temperature range is completely reversible. At 64°C, only a shallow trough from 270 to 272 nm is apparent with a rather weak shoulder at 280 nm. Heating above 64°C leads to complete disruption of the apoB-NaDC micelle and irreversible protein unfolding.

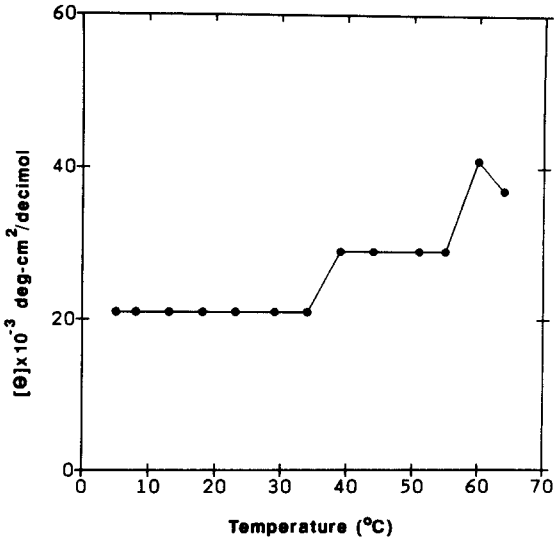

Fig. 6. Molar ellipticity at 290 nm versus temperature for apoB in LDL.

DISCUSSION

Calorimetric measurements of proteins represent the only method available for the direct measurement of the enthalpy associated with temperature-induced changes in state of a protein (30–32). Calorimetric studies have revealed important information on the structural and functional domains in fibrinogen (39), prothrombin (40), plasminogen (41), and fibronectin (42). The folding-unfolding process of proteins or domains of proteins is generally a highly cooperative process, but, the physical reasons governing this process are not completely clear.

LDL, the native lipid environment of apoB, represents a complex chemical milieu in which apoB is solubilized in a lipid "microemulsion" particle (2, 3, 43). The micellar particle of apoB solubilized in NaDC is a less complex system than the native lipid environment of LDL. However, apoB maintains many of its native characteristics solubilized in NaDC (11, 18).

LDL

From 5 to 40°C, a temperature range encompassing the CE order-disorder transition, both far (11, 44, 45) and near UV-CD spectroscopy have shown that both the secondary and tertiary structural organizations of apoB in LDL are unaltered, undergoing no detectable conformational changes (Fig. 2, inset; Figs. 5 and 6).

Between 48 and 57°C, a previously unreported thermal event is detected by high resolution calorimetry. This re-

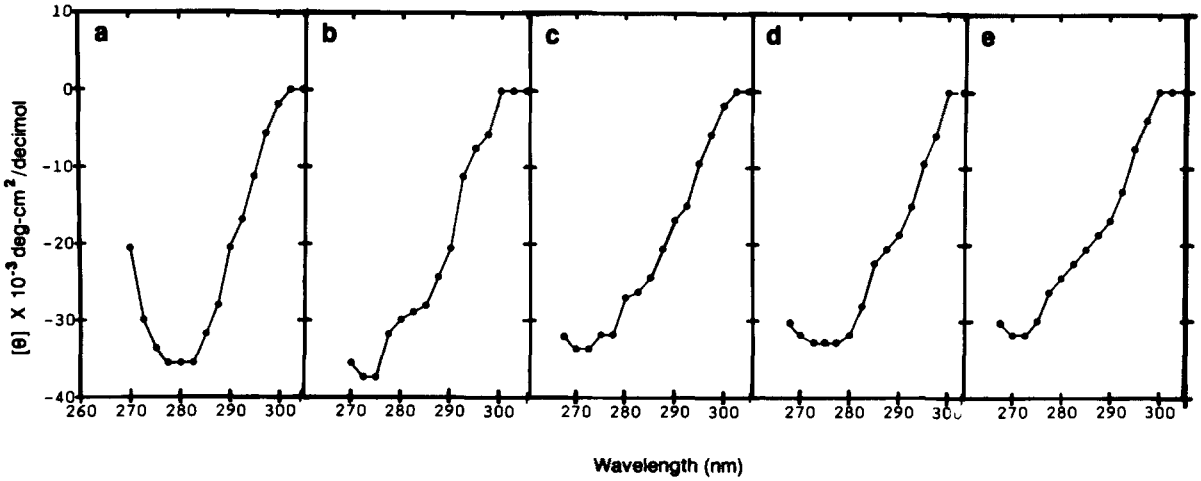

Fig. 7. Near UV circular dichroic spectra of apoB solubilized in NaDC. ApoB-NaDC samples were ~2 mg apoB/ml in 50 mM NaCl, 50 mM sodium carbonate, 10 mM NaDC, 0.02% NaN_3, pH 10. Cell pathlength was 1.0 cm. See * in legend for Fig. 5 (see Methods for experimental details); (a) 7°C; (b) 42°C; (c) 49°C; (d) 55°C; (e) 64°C.

versible transition has a ratio of $\Delta H/\Delta H_{vH}$ of unity, suggesting that the entire apoB molecule is undergoing a reversible structural reorganization in a cooperative manner over this temperature range. Far UV-CD studies show no alteration in the secondary structure of apoB (Fig. 2, inset, and ref 11) in this temperature range. However, the near UV-CD data presented in these studies suggest that an alteration in the tertiary structural organization of apoB does occur at temperatures coinciding with this thermal event.

In the wavelength range of 270 to 290 nm of the near UV region, Tyr, Trp, Phe, and disulfide bonds absorb (38, 46, 47). While it is not possible at this time to assign a positive identity at a molecular level to the maximum observed at 290 nm in the near UV-CD spectrum, both the magnitude and wavelength of the maximum are altered in response to temperature and correlate with the reversible thermodynamic events observed by calorimetry. This low enthalpy thermal event may thus result from a cooperative reversible change in the tertiary structure of apoB over this temperature range.

Calorimetry has previously shown (2, 3) that an irreversible transition occurs in LDL from ~65–80°C. This has been attributed to disruption of the LDL particle and protein unfolding-denaturation.

Thus, apoB in LDL undergoes two separate thermal events: *1*) the first is reversible and coincides with an alteration in the tertiary structure of apoB as shown by near UV-CD; *2*) the second is irreversible and may involve lipid-associated regions of the apoB molecule whose unfolding-disruption-denaturation may hinder the refolding or reannealing of apoB to its native state.

ApoB solubilized in NaDC

The unfolding of apoB solubilized in NaDC proceeds through a multi-stage melting, suggesting the presence of domains (Figs. 3 and 4; Table 2). In NaDC the unfolding process involves at least three stages, the first two of which are reversible and occur between 40 and 60°C. The ratio of $\Delta H/\Delta H_{vH}$ for these transitions of apoB solubilized in NaDC have values greater than unity, indicating that each of the thermal events may not be a single two-state process, but may be composed of a number of intermediate two-state processess, possibly due to the existence of independent structural domains.

Deconvolution of the two reversible transitions confirms that apoB may be undergoing a number of two-state thermal events. The lower temperature reversible transition (T_m = 44.9°C) is predominated by one event comprising ~28% of the ΔH of both reversible peaks as well as portions of other two-state events. These include an intermediate temperature transition T_m 49.5°C, representing 19% of the total ΔH. Three peaks comprising 16, 20, 17% of the total enthalpy, respectively, occur at very similar temperatures. The findings suggest quite strongly that the reversible thermal transitions observed in apoB solubilized in NaDC may result from separate thermal events of specific regions of apoB that melt over a discrete temperature range and overlap to some extent with the melting of other regions.

Between 40 and 60°C, as shown by us previously (11) and presented briefly here (Fig. 4, inset), far UV-CD studies also detect a reversible alteration in the secondary structure of apoB, specifically a decrease in the amount of β-sheet and a concomitant increase in random coil. The near UV-CD measurements presented here also show a reversible structural change in this temperature range, suggesting that, in addition to the changes observed in secondary structure (11), there is also an alteration in the tertiary structure of apoB. Cardin et al. (48) have shown that delipidated apoB under water-soluble, detergent-free, nonreducing conditons exhibits a near UV-CD

spectrum similar to that shown in Fig. 7a with a negative minimum at ~275 nm and a simlar molar ellipticity. Their study has clearly demonstrated that with preparations of apoB that were carboxyamidomethylated, reduced and carboxyamidomethylated, or reduced, the position and magnitude of this peak is highly dependent on the state of the disulfide bonds. The near UV-CD spectrum of apoB is thus dependent on the inter- and intramolecular disulfide bonds of apoB which may produce conformational constraints and ultimately influence the environment of the aromatic residues.

Heating above 65°C results in the irreversible loss of the native secondary and tertiary structures of apoB and micelle disruption. This final irreversible unfolding may represent the disruption of those regions of the apoB molecule intimately involved in the binding of NaDC.

The observation that the thermal unfolding of apoB, either in LDL or solubilized in NaDC, is not a simple two-stage process is not surprising in view of the high molecular weight of apoB and its potential organization into various regions in native LDL (totally extra-particle, lipid binding, non-lipid binding, receptor binding) (10).

The differences between near UV-CD spectra, particularly the 275-295 nm region, of apoB in LDL and NaDC recorded at similar temperatures reflect the overall differences in the tertiary and quasi-quaternary structure of apoB in these different environments.

There are several possible reasons for these differences. The environments that apoB is experiencing are quite different in the two systems. In LDL, the presence of both polar and nonpolar lipids may potentially provide the appropriate environments for both hydrophobic and hydrophilic amino acids. In contrast, apoB solubilized in NaDC (a weakly ionic detergent) is not presented with the opportunity to partition into regions of different polarity. The particle sizes and their shapes are quite different. LDL is a spherical particle with a diameter of 220 Å (39) while the micellar particle with NaDC has been reported to be a prolate ellipsoid with a particle radius of ~120 Å and an axial ratio of 5.6 (49). However, although their particle morphologies are quite different, the overall secondary structures of apoB in either the polar or nonpolar environments are very similar at least from 0-30°C (11). Tyr, Trp, and Phe residues of apoB, although at some temperatures in a similar secondary structural region, may lie in a different tertiary structure. The dihedral angles of the disulfide bridges may be altered.

In conclusion, the melting of apoB in either LDL or solubilized in NaDC proceeds through a number of discrete stages, each associated with a significant ethalpy effect. The magnitude of these changes demonstrates that each of these stages corresponds to some conformational or structural change in apoB.

The multistage character of the melting of apoB indicates that the unfolding of apoB in both LDL and NaDC micelles cannot be explained as a single simple two-state process or sequential transformation of the entire apoB molecule but as various regions of the molecule undergoing separate melting processes. This suggests that apoB does not represent a single cooperative unit, but a system consisting of regions or domains that behave, at least partially, independently.

This work was supported by U. S. Public Health Service Grant HL-26335.

Manuscript received 19 October 1989.

REFERENCES

1. Brown, M. S., and J. L. Goldstein. 1976. Receptor-mediated control of cholesterol metabolism. *Science.* **191:** 150-154.
2. Deckelbaum, R. J., G. G. Shipley, D. M. Small, R. S. Lees, and P. K. George. 1975. Thermal transitions in human plasma low density lipoproteins. *Science.* **190:** 392-394.
3. Deckelbaum, R. J., G. G. Shipley, and D. M. Small. 1977. Structure and interactions of lipids in human plasma low density lipoproteins. *J. Biol. Chem.* **252:** 744-754.
4. Ginsburg, G. S., D. M. Small, and D. Atkinson. 1982. Microemulsions of phospholipids and cholesterol esters: protein-free models of low density lipoproteins. *J. Biol. Chem.* **257:** 8216-8227.
5. Basu, S. K., R. G. W. Anderson, J. L. Goldstein, and M. S. Brown. 1977. Metabolism of cationized lipoproteins by human fibroblasts. *J. Cell Biol.* **74:** 119-135.
6. Mahley, R. W., and T. L. Innerarity. 1978. Sixth International Symposium on Drugs Affecting Lipid Metabolism. D. Kritchevsky, R. Paoletti, and W. L. Holmes, editors. Plenum Press, New York. 99-127.
7. Knott, T. J., L. M. Pease, L. M. Powell, S. C. Wallis, S. C. Rall, Jr., T. L. Innerarity, B. Blackhart, W. H. Taylor, Y. Marcel, R. Milne, D. Johnson, M. Fuller, A. J. Lusis, B. J. McCarthy, R. W. Mahley, B. Levy-Wilson, and J. Scott. 1986. Complete protein sequence and identification of structural domains of human apolipoprotein B. *Nature.* **323:** 734-738.
8. Cladaras, C., M. Hadzopoulou-Cladaras, R. T. Nolte, D. Atkinson, and V. I. Zannis. 1986. The complete sequence and structural analysis of human apolipoprotein B-100: relationship between apoB-100 and apoB-48 forms. *EMBO J.* **5:** 3495-3507.
9. Yang, C. Y., S-H. Chen, S. H. Gianturco, W. A. Bradley, J. T. Sparrow, M. Tanimura, W-H. Li, D. A. Sparrow, H. DeLoof, M. Rosseneu, F-S. Lee, Z-W. Gu, and A. M. Gotto, Jr. 1986. Sequence, structure, receptor-binding domains and internal repeats of human apolipoprotein B-100. *Nature.* **323:** 738-742.
10. Yang, C. Y., Z-W. Gu, S. Weng, S. H. Chen, H. J. Pownall, P. M. Sharp, S-W. Liu, W-H. Li, A. M. Gotto, Jr., and L. Chan. 1989. Structure of apolipoprotein B-100 of human low density lipoproteins. *Arteriosclerosis.* **9:** 96-108.
11. Walsh, M. T., and D. Atkinson. 1986. Physical properties of apoprotein B in mixed micelles with sodium deoxycholate and in a vesicle with dimyristoyl phosphatidylcholine. *J. Lipid Res.* **27:** 316-325.
12. Privalov, P. L. 1982. Stability of proteins. Proteins which do not present a single cooperative system. *Adv. Protein Chem.* **35:** 1-104.
13. Krishnan, K. S., and J. F. Brandts. 1978. Scanning calorimetry. *Methods Enzymol.* **49:** 3-14.

14. Cardin, A. D., K. R. Witt, J. Chao, H. S. Margolius, V. H. Donaldson, and R. L. Jackson. 1984. Degradation of apolipoprotein B-100 of human plasma low density lipoproteins by tissue and plasma kallikreins. *J. Biol. Chem.* **259:** 8522–8528.
15. Havel, R. J., J. A. Eder, and J. H. Bragdon. 1955. The distribution and chemical composition of ultracentrifugally separated lipoproteins in human serum. *J. Clin. Invest.* **34:** 1345–1353.
16. Noble, R. P. 1968. Electrophoretic separation of plasma lipoproteins in agarose gel. *J. Lipid Res.* **9:** 693–700.
17. Steele, J. C. H., and J. A. Reynolds. 1979. Characterization of the apolipoprotein B polypeptide of human plasma low density lipoprotein in detergent and denaturant solutions. *J. Biol. Chem.* **54:** 1633–1638.
18. Walsh, M. T., and D. Atkinson. 1983. Solubilization of low-density lipoprotein with sodium deoxycholate and recombination of apoprotein B with dimyristoylphosphatidylcholine. *Biochemistry.* **22:** 3170–3178.
19. Laemmli, U. K. 1970. Cleavage of structural proteins during the assembly of the head of bacteriophage T4. *Nature.* **227:** 680–685.
20. Lowry, O. H., N. J. Rosebrough, A. L. Farr, and R. J. Randall. 1951. Protein measurement with the Folin phenol reagent. *J. Biol. Chem.* **193:** 265–275.
21. Markwell, M. A. K., S. M. Haas, L. L. Bieber, and N. E. Tolbert. 1978. A modfication of the Lowry procedure to simplify protein determination of membrane and lipoprotein samples. *Anal. Biochem.* **87:** 206–210.
22. Greenfield, N., and G. D. Fasman. 1969. Computed circular dichroism spectra for the evaluation of protein conformation. *Biochemistry.* **8:** 4108–4116.
23. Morrisett, J. D., J. S. K. David, H. Pownall, and A. M. Gotto. 1973. Interaction of an apolipoprotein (apoLP-alanine) with phosphatidylcholine. *Biochemistry.* **12:** 1290–1299.
24. Smith, R., J. R. Dawson, and C. R. Tanford. 1972. The size and number of polypeptide chains in human serum low density lipoprotein. *J. Biol. Chem.* **247:** 3376–3381.
25. Freire, E., and R. L. Biltonen. 1978. Statistical mechanical deconvolution of thermal transitions in macromolecules. I. Theory and application to homogenous systems. *Biopolymers.* **17:** 463–479.
26. Freire, E., and R. L. Biltonen. 1978. Statistical mechanical deconvolution of thermal transitions in macromolecules. II. General treatment of cooperative phenomena. *Biopolymers.* **17:** 481–496.
27. Freire, E., and R. L. Biltonen. 1978. Statistical mechanical deconvolution of thermal transitions in macromolecules. III. Application to double-stranded to single-stranded transitions of nucleic acids. *Biopolymers.* **17:** 497–510.
28. Rigell, C. W., C de Saussure, and E. Freire. 1985. Protein and lipid structural transitions in cytochrome c oxidase-dimyristoylphosphatidylcholine reconstitutions. *Biochemistry.* **24:** 5638–5646.
29. Fukada, H., J. M. Sturtevant, and F. A. Quiocho. 1983. Thermodynamics of the binding of L-arabinose-and D-galactose to the L-arabinose-binding protein of *Escherichia coli*. *J. Biol. Chem.* **258:** 13193–13198.
30. Biltonen, R. L., and E. Freire. 1978. Thermodynamic characterization of conformational states of biological macromolecules using differential scanning calorimetry. *CRC Crit. Rev. Biochem.* **5:** 85–124.
31. Privalov, P. L., and N. N. Khechinashvili. 1974. A thermodynamic approach to the problem of stabilization of globular protein structure: a calorimetric study. *J. Mol. Biol.* **86:** 665–684.
32. Privalov, P. L., and S. A. Potehkin. 1986. Scanning microcalorimetry in studying temperature-induced changes in proteins. *Methods Enzymol.* **131:** 4–51.
33. Swaminathan, N., and F. Aladjem. 1976. The monosaccharide composition and sequence of the carbohydrate moiety of human serum low density lipoproteins. *Biochemistry.* **15:** 1516–1522.
34. Lee, P., and W. C. Breckinridge. 1976. Isolation and carbohydrate composition of glycopeptides of human apo low-density lipoprotein from normal and type II hyperlipoproteinemic subjects. *Can. J. Biochem.* **54:** 829–833.
35. Siuta-Mangnao, P., S. C. Howard, W. J. Lennarz, and M. D. Lane. 1982. Synthesis, processing, and secretion of apolipoprotein B by the chick liver cell. *J. Biol. Chem.* **257:** 4292–4300.
36. Vauhkonen, M., J. Viitala, J. Parkinnen, and H. Rauvala. 1985. High-mannose structure of apolipoprotein-B from low-density lipoproteins of human plasma. *Eur. J. Biochem.* **152:** 43–50.
37. Walsh, M. T., J. A. Hamilton, D. Atkinson, and D. M. Small. 1988. Secondary and tertiary structure of apolipoproteins. *In* Eicosanoids, Apolipoproteins, Lipoprotein Particles and Atherosclerosis. C. L. Malmendier, editor. Plenum Publishing Co., New York, NY.
38. Sears, D. W., and S. Beychok. 1973. Circular dichroism. *In* Physical Principles and Techniques of Protein Chemistry. Part C. S. J. Leach, editor. Academic Press, New York. 445–593.
39. Donovan, J. W., and E. Mihalyi. 1974. Conformation of fibrinogen: calorimetric evidence for a three-nodular structure. *Proc. Natl. Acad. Sci. USA.* **71:** 4125–4128.
40. Ploplis, V. A., D. K. Strickland, and F. J. Castellino. 1981. Calorimetric evaluation of the existence of separate domains in bovine prothrombin. *Biochemistry.* **20:** 15–21.
41. Castellino, F. J., V. A. Ploplis, J. R. Powell, and D. K. Strickland. 1981. The existance of independent domain structures in human Lys_7-plasminogen. *J. Biol. Chem.* **256:** 4778–4782.
42. Niedzwiadek, W. E., G. T. O'Bryan, F. A. Blumenstock, T. M. Saba, and T. T. Andersen. 1988. A calorimetric analysis of human plasma fibronectin: effects of heparin binding on domain structure. *Biochemistry.* **27:** 7116–7124.
43. Ginsburg, G. S., M. T. Walsh, D. M. Small, and D. Atkinson. 1984. Reassembled plasma low density lipoproteins. *J. Biol. Chem.* **259:** 6667–6673.
44. Scanu, A., H. Pollard, R. Hirz, and K. Kothary. 1969. On the conformational instability of human serum low-density lipoprotein: effect of temperature. *Proc. Natl. Acad. Sci. USA.* **62:** 171–178.
45. Dearborn, D. G., and D. B. Wetlaufer. 1969. Reversible thermal conformation changes in human serum low-density lipoprotein. *Proc. Natl. Acad. Sci. USA.* **62:** 179–185.
46. Mandal, K., B. Chakrabarti, J. Thomson, and R. J. Siezen. 1987. Structure and stability of γ-crystallins. *J. Biol. Chem.* **262:** 8096–8102.
47. Wharton, S. A., R. W. H. Ruigrok, S. R. Martin, J. J. Skehel, P. M. Bayley, W. Weiss, and D. C. Wiley. 1988. Conformational aspects of the acid-induced fusion mechanism of influenza virus hemagglutinin. *J. Biol. Chem.* **263:** 4474–4480.
48. Cardin, A. D., K. R. Witt, C. L. Barnhart, and R. L. Jackson. 1982. Sulfhydryl chemistry and solubility properties of human plasma apolipoprotein B. *Biochemistry.* **21:** 4503–4511.
49. Oeswein, J. Q., and P. W. Chun. 1983. Human serum low density lipoprotein-sodium deoxycholate interaction. *J. Biol. Chem.* **258:** 3645–3654.

50. Lee, D. M., and S. Singh. 1988. Presence and localization of two intramolecular thiolester linkages in apolipoprotein B. *Circulation.* **78:** II-286.
51. Huang, G., D. M. Lee, and S. Singh. 1988. Identification of the thiol ester-linked lipids in apolipoprotein B. *Biochemistry.* **27:** 1395-1400.
52. Helenius, A., and K. Simons. 1971. Removal of lipids from human plasma low density lipoprotein by detergents. *Biochemistry.* **10:** 2542-2547.
53. Hirs, C. H. W. 1967. Reduction and S-carboxymethylation of proteins. *Methods Enzymol.* **22:** 199-203.